LC-TH-2001-031

Forward jets as a BFKL signature at an e^+e^- or $e\gamma$ linear collider

J. G. Contreras
Departamento de Física Aplicada, CINVESTAV–IPN, Unidad Mérida, A. P. 73
Cordemex, 97310 Mérida, Yucatán, México

A. De Roeck
CERN, 1211 Geneva 23, Switzerland

Abstract

The measurement of forward jets in DIS $e\gamma$ events is studied for a future linear e^+e^- collider, both for the ee mode and the $e\gamma$ mode. These measurements are sensitive to BFKL effects, as was demonstrated by HERA.

1 Introduction

The electron-proton collider HERA has opened new kinematic regions to study Deep Inelastic Scattering (DIS): the regions of large four-momentum transfer Q^2 (up to $Q^2 \approx 10^4$ GeV^2) and small Bjorken-x ($x \approx 10^{-4}$). The region of small x is sensitive to new dynamic features of QCD [1]. The debate is whether the QCD evolution of the parton densities can be described by the DGLAP (Dokshitzer-Gribov-Lipatov-Altarelli-Parisi) [2] evolution equations, or whether they extend into a new regime where the QCD dynamics is described by the BFKL (Balitsky-Fadin-Kuraev-Lipatov) [3] evolution equation. The BFKL evolution equation is expected to become applicable in the region at small x, since it resums all $\ln 1/x$ terms in the perturbative expansion, contrary to the DGLAP equation.

For events at low x, hadron production in the region between the current jet and the proton remnant is expected to be sensitive to effects of the BFKL or DGLAP dynamics [4, 5]. At lowest order the BFKL and DGLAP evolution equations effectively resum the leading logarithms $\alpha_s \ln 1/x$ or $\alpha_s \ln Q^2$ contributions respectively which, in an axial gauge, amounts to a resummation of ladder diagrams of the type shown in Fig. 1. It shows that before a quark is struck by the virtual photon, a cascade of partons may be emitted. The proton momentum fractions x_i and transverse momenta k_i of the emitted partons are indicated in the figure. In the leading log DGLAP scheme this parton cascade follows a strong ordering in transverse momentum $k_n^2 \gg k_{n-1}^2 \gg ... \gg k_1^2$, while there is only a soft (kinematical) ordering for the fractional momentum $x_n < x_{n-1} < ... < x_1$. For the BFKL scheme the cascade follows a strong ordering in fractional momentum $x_n \ll x_{n-1} \ll ... \ll x_1$, while there is no ordering in transverse momentum [6]. The transverse momentum follows a kind of random walk in k space: the k_i value is close to the k_{i-1} value, but it can be both larger or smaller [7].

2 Forward jets at HERA

A possible footprint of the BFKL dynamics is the rate of jets produced in DIS, with the following characteristics [4, 5, 8], designed to suppress the phase space for jet production resulting from the DGLAP evolution compared to the one in case of BFKL evolution. A first requirement is the condition $k_J^2 \approx Q^2$ which, due to the strong ordering, leaves little room for DGLAP evolution. The momentum fraction of the jet, $x_J = E_{\rm jet}/E_p$, should be as large as possible, whereas the momentum fraction x of the quark struck by the virtual photon should be small, in order to maximize the phase space for jet production from BFKL evolution which is governed by the ratio x_J/x. Here $E_{\rm jet}$ and E_p are the energies of the jet and the incoming proton respectively. Hence the rate of events at small x with a jet at high x_J is expected to be higher for the BFKL than for the DGLAP scenario.

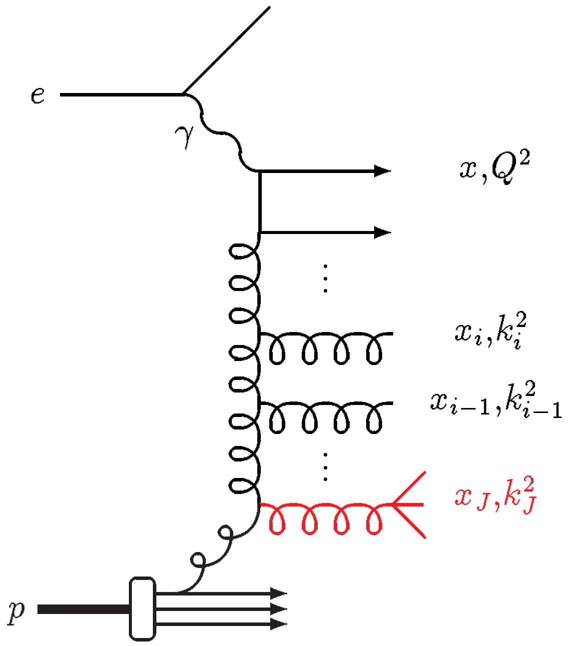

Figure 1: Representation of a deep inelastic event using a physical gauge within perturbative QCD.

The process selected has a well defined experimental topology. A DIS event is selected with a jet at high rapidity and the virtuality of the proton is choosen to be of the same magnitude as the transverse momentum squared of the jet. Since the direction of the proton is termed by the HERA experiments the forward direction, this kind of events are known as forward jets events.

Recently both the H1 [12] and the ZEUS [13] collaborations have presented cross sections for this observable. The H1 collaboration selects DIS events requiring the energy (E_e) and polar angle (θ_e) of the scattered electron to be $E_e > 11$ GeV and $160^\circ < \theta_e < 173^\circ$. ZEUS only requires $E_e > 10$ GeV and the polar angle θ_e is restricted by the rest of the kinematic constrains. Both of them select events with $y_{Bj} > 0.1$ to avoid the jet from the struck quark going forward. In the jet side, selected with a cone algorithm of radius 1, the cuts used are for H1: $k_J > 3.5$ GeV, $x_J \approx E_J/E_{beam} = E_J/820\text{GeV} > 0.035$ and $7^\circ < \theta_J < 20^\circ$. ZEUS requires jets with $k_J > 5.0$ GeV, $x_J > 0.036$ and $8.5^\circ < \theta_J$. Both collaborations require that $0.5 < k_J^2/Q^2 < 2.0$.

Samples of a few 1000 events with forward jets have been analysed. The result of these measurements is that none of the DGLAP based models is capable to describe the data. All of them – NLO matrix element calculations (ME) at the parton level [14] and LO ME plus parton showers with and without coherence and a hadronization prescription [15, 16] – lie significantly below the data.

On the other hand, BFKL type calculations are closer to the data [17, 18, 19]. Using two DGLAP ladders [20], one from the photon and one from the proton side, can describe the present jet data, but it can not describe the latest data form H1 on forward pions [21]. A BFKL calculation however can describe the jet and pion data [18].

3 Forward jets at a linear collider

The DIS process discussed above is not limited to ep scattering, but is also realized in $e\gamma$ scattering, i.e the proton is replaced by a resolved photon. DIS $e\gamma$ scattering is studied in two-photon processes, at electron-positron colliders.

Two photon processes at future high energy linear colliders such as TESLA, can be measured either as in a storage ring, via photon emission from the lepton beams, according to a Weizsäcker Williams(WW)[9] energy distribution, or using the LC in a photon collider mode [10]. In the latter case the high energy electron beam is converted into a high energy photon beam, by backscattering of photons of an intense laser beam, just before the interaction point.

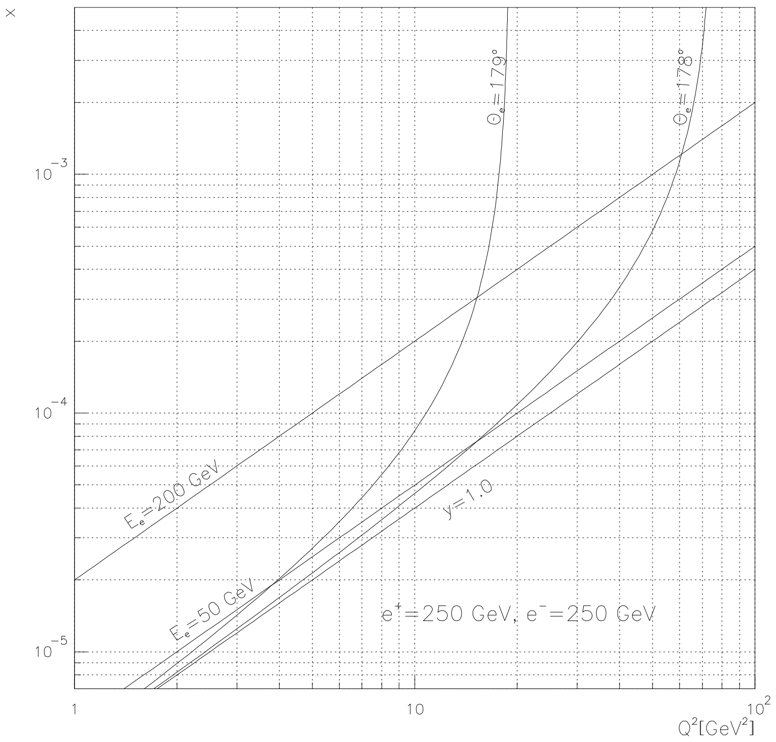

Figure 2: The kinematics of $e\gamma$ DIS, shown for the scattered electron angle and energy.

The maximum energy of the generated photons is given by $E_\gamma^{max} = xE_e/(1+x)$, with E_e the electron beam energy and $x = 4E_eE_L\cos^2(\theta/2)/m_e^2c^4$ with E_L and θ the laser photon energy and angle between the electron and laser beam. The distance of the conversion to the interaction point is in the range of several mm to a few cm. A typical value for x is 4.8, which leads to photon spectra which peak around $0.8E_e$. Hence converting only one beam leads to $e\gamma$ collisions with a typical luminosity distribution as a function of the invariant mass peaking at the maximum reachable invariant mass of around $0.9\sqrt{s_{e^+e^-}}$ with widths of $\approx 10\%$. The 'luminosity' is usually defined to be the luminosity corresponding to the region $0.8\sqrt{s_{e\gamma,max}} < \sqrt{s_{e\gamma}} < \sqrt{s_{e\gamma,max}}$

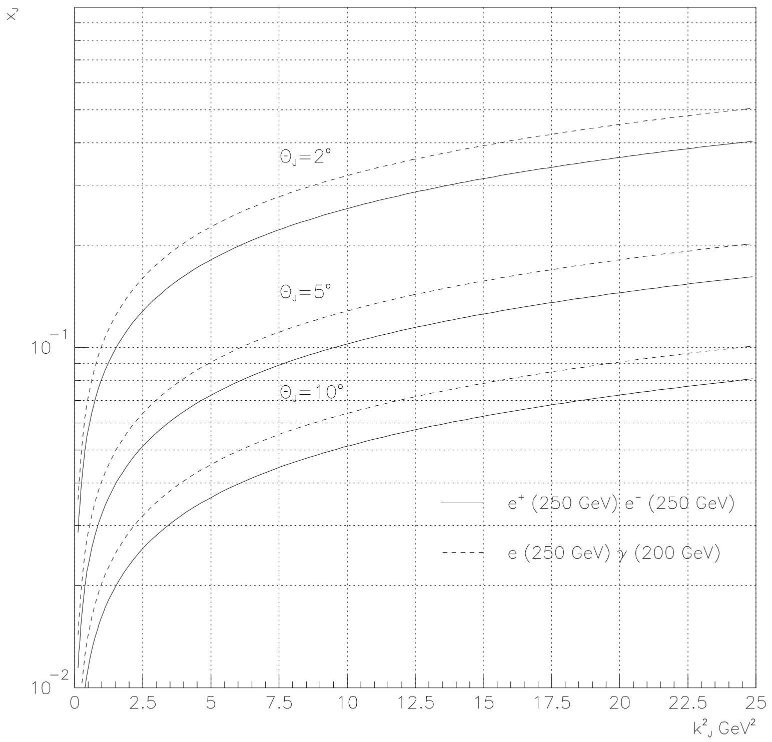

Figure 3: The angle of the forward jet as function of its transverse momentum k^2 and x_J, for an ee and $e\gamma$ collider.

and is typically 10% of the geometrical e^+e^- luminosity $\mathrm{L}_{\mathrm{geom}}$. However, since the electron beams are converted before collision, smaller β functions at the interaction point can be allowed for. This can make up for part of the luminosity lost compared to an e^+e^- collider, by using smaller beam spots. For TESLA [11] one finds $\mathrm{L}_{e\gamma} \simeq 0.1 - 0.3\mathrm{L}_{e^+e^-}$ This leads to event samples corresponding of order 100 fb^{-1} per year for the photon collider.

The energy and kinematics of $e\gamma$ scattering at a future linear collider is such that forward jet production processes become accessible. Hence in the lower part of the diagram in Fig.1, the proton gets replaced by a (resolved) photon, coming either from Bremsstrahlung off the $e^\pm$ leg (e^+e^- LC) or from Compton backscattering ($e\gamma$ LC), without changing the character of the process as a BFKL signature.

The cross section of this process in a e^+e^- LC has the same form than that for the HERA case, which has been calculated in [8, 22, 23, 24]. There are two changes needed: to use the structure functions of the photon instead of the proton, and to take into account the Bremsstrahlung off the lepton line. The $e\gamma$ LC scenario is even simpler because the factor due to the photon Bremsstrahlung does not appear.

The differential cross section then reads:

$$k_J^2 x_J \frac{d^5\sigma}{dydQ^2dx_Jdk_J^2dy_\gamma} = C\alpha_s\sqrt{\frac{Q^2}{k_J^2}} f_{\gamma/e}(y_\gamma)F_\gamma(x_J/y_\gamma, k_J^2)\frac{\exp[(\alpha_p - 1)\ln x_J/x]}{(\ln x_J/x)^2} \tag{1}$$

for the e^+e^- LC case, and

$$k_J^2 x_J \frac{d^4\sigma}{dydQ^2dx_Jdk_J^2} = C\alpha_s\sqrt{\frac{Q^2}{k_J^2}} F_\gamma(x_J, k_J^2)\frac{\exp[(\alpha_p - 1)\ln x_J/x]}{(\ln x_J/x)^2} \tag{2}$$

for the $e\gamma$ LC. Here C is a numerical constant, α_s has been evaluated at $\max(Q^2, k_J^2)$ and

$$F_\gamma(x_J, Q^2) = x_J G_\gamma(x_J, Q^2) + \frac{4}{9}[x_J q_\gamma(x_J, Q^2) + x_J \bar{q}_\gamma(x_J, Q^2)] \tag{3}$$

where the GRV structure functions of the photon were used [25], for 3 flavours. As for the forward jet production at HERA, a factor 1.2 was included to take charm into account. The formulae of [8] are in leading order.

The kinematic coverage for measurements of $e\gamma$ scattering strongly depends on the minimal angle $\theta_{\text{tag,min}}$ down to which the scattered electron can be detected. An electron tagger inside the radiation shielding masks of the main detector in its present design accepts electrons down to $\theta_{\text{tag,min}} = 25$ mrad. Equally important is the background suppression cut $E_{\text{tag,min}}$ on the energy of the scattered electron, for which $E_{\text{tag,min}} = 50$ GeV is considered to be feasible.

At first sight, the kinematic plane for this measurement is more or less the same as for HERA (see Fig. 2). The main change is a factor 2.5 increase in center of mass energy, which allows to measure down to $x = 10^{-4}$ and below. On the electron side, the energy of the electron to be tagged is substantially larger: at HERA the electrons at $Q^2 \approx 10$ GeV have energies under 30 GeV. In the LC electrons will be selected with energies from 20 to 50 GeV onwards to 250 GeV.

An advantage of a LC with respect to HERA is that there is almost no event boost. Hence the forward jets will be produced more centrally, away from the edge of the polar acceptance of the detectors, facilitating the experimental detection. Reversely, it means that with the same laboratory angle than at HERA a factor 3 bigger x_J will be reached. The kinematics of the forward jet in a LC is shown in Fig. 3. The angle of the forward jet as function of its transverse momentum k_J^2 and x_J, for an ee and $e\gamma$ collider is shown.

There is an additional degree of freedom to transform from the $e\gamma$ frame to the laboratory frame [8]. The angle between the produced forward jet and the virtual photon is not determined. For Fig. 3 this angle was set to $\pi/2$. Variation of this angle produces changes in the reached x_J up to a factor of around 3 upwards.

Furthermore, the luminosity for the planned LC's are about a factor 100-1000 higher than at HERA, leading additionally to large event rates.

4 Results and Discussion

To study the feasibility of such measurement the eqns. 1,2 have been integrated numerically imposing possible realistic detector cuts. The cuts have been inspired by the analyses presently ongoing at HERA. These cuts have been varied in the following to explore possible improvements of the channel, with more challenging detector requirements. The detector cuts used were:

- For the scattered electron: $0.1 < y < 0.95$, to ensure good kinematic reconstruction; $\theta_e < 178°$ for a good acceptance; $E_e > 50$ GeV for a good efficiency and triggering.

- For the jet : $5° < \theta_J < 20°$ for good acceptance (lower cut) and separation to the struck quark jet (upper cut); $k_J > 4$ GeV to ensure

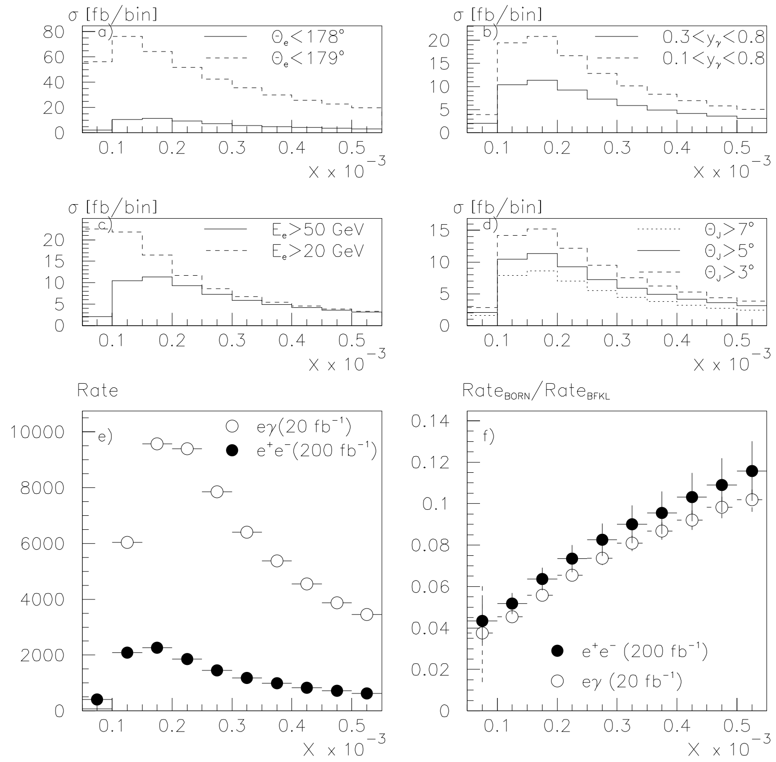

Figure 4: The forward jet cross section given in pb/bin for the standard cuts for the ee mode (solid line/full points), compared with cross sections with modified cuts (a-d), and compared with the $e(250\text{GeV})\gamma(200\text{GeV})$ mode (open points) e). Also shown is the ratio of the Born to BFKL cross section for both cases (f).

an efficient reconstruction of jet variables and $x_J > 0.05$ to enlarge the phase space in x as much as possible; $0.5 < k_J^2/Q^2 < 2.0$ for selecting forward jets events with the photon virtuality close to the jet p_T to suppress DGLAP evolution.

- For the e^+e^- mode only: The electron which emits the resolved photon is in the region $0^\circ < \theta_e < 1^\circ$, and thus will not be tagged in the instrumented mask. The $y_\gamma = E_\gamma/E_b$ range of the real photon for the ee option is measured either by a downstream zero angle electron tagger (to detect the electron that emitted the real photon), if technically feasible, or by reconstructing the hadronic final state of the interaction in the central detector. In case of the latter the resulution on this quantity and hence the reconstruction of x will be relatively poor. In these calculations $0.3 < y_\gamma < 0.8$ is choosen.

The forward jet cross section for a e^+e^- LC with the above cuts is shown as the solid histogram of Fig. 4 a) to d). The cross section rises with decreasing x. The drop in the lowest x bin is a consequence of the phase space cuts.

With the given cuts the minimum Q^2 value of the DIS event is 20 GeV^2, and lowest x range is slightly lower than 10^{-4}. For an e^+e^- collider with 100 fb^{-1}/year, the event rates are of order a few 10^3 events per bin in one year of data taking.

Several cuts have been varied.

- The $\theta_e < 178°$ (35 mrad) was changed to 179° (17.5 mrad): this results in a factor 7 increase in the statistics, and an increased reach at small x by a factor 3. Hence an as low as possible tagging angle will be important for this measurement.

- Reducing E_e from 50 to 20 GeV: a gain in low x of about a factor 2 and one bin at lower x. The slope of change of the the cross section with decreasing x suffers considerably less the phase space restrictions at low x, and will be easier to determine. This cut will depend on the machine background.

- Reducing/increasing the cut on θ_J: only a modest change in the statistics, which implies that one could adopt a more relaxed cut (e.g. 7°) without significant loss in sensitivity to the BFKL effect.

- The y_γ range of the real photon is enlarged, showing mostly an increased cross section, but no strong improvement in the kinematic reach.

Finally, there are several advantages using the $e\gamma$ option. The energy of the real photon is known (within 10%) hence the variable x can be directly reconstructed from the scattered electron as in DIS at HERA. Further, the cross section increases on average by a factor of 50. This will be partially lost (factor 3-10) by the lower luminosity of the $e\gamma$ collider, but a gain remains.

The kinematical reach is somewhat reduced (one bin in our analysis). In Fig. 4 the event rates are compared for both colliders, with the same event selection cuts. The luminosity of the photon collider was taken to be 10% of that of a ee collider, which is at the pessimistic side. Note that for the photon collider option one looses the lowest x bin, compared to the ee collider.

The ratio Born/BFKL is also shown in Fig. 4. Here 'Born' is the 2-gluon exchange diagram, i.e. the diagram that does not contain BFKL evolution effects. For all cross sections with the different cuts the ratio Born/BFKL is about the same and found to be around 0.1 for high x, decreasing linearly to about 0.04 at the lowest x bin. This means that it will be easy to see the onset of BFKL effect. This ratio (in other words the BFKL cross section) is very sensitive to the effective power α_{bfkl} of the s dependence in the cross section. In leading order this amounts to $\alpha_{bfkl} = 0.5$. Meanwhile it is known that the higher order corrections to the BFKL evolution are significant, and values $\alpha_{bfkl}^{HO} = 0.2 - 0.3$ are found for some processes. Hence the cross section of the BFKL will be smaller, but still a factor of 2-3 larger than the Born cross section. A detailed estimation of this higher order effect is the subject of a forthcoming note.

5 Conclusion

Forward jet production has been studied for the ee and $e\gamma$ modes. for a future high energy linear collider, both of which will allow this process to be studied. The higher energy and better acceptance at a LC make this process more easily accessible at an LC than at HERA. The reach to lower x is increased compared to HERA. Low angle electron tagging is essential for both modes. The event rates are large and will allow a detailed study of the onset (or absence) of BFKL in the regime of $x \sim 10^{-4}$.

6 Acknowledgments

We wish to thank Mark Wueshoff for his help with the BFKL program. J.G.C. thanks the support by CONACyT Mexico.

References

[1] J. Bartels and J. Feltesse, Proceedings of the Workshop *Physics at HERA*, ed. W. Buchmüller and G. Ingelman, Hamburg (1992) 133;
E.M. Levin, Proc. QCD – 20 Years Later, eds. P.M. Zerwas and H.A. Kastrup, Aachen (1992), vol. 1, p. 310.

[2] Yu. L. Dokshiter, Sov. Phys. JETP 46 (1977) 641;
V. N. Gribov and L. N. Lipatov, Sov. J. Nucl. Phys. 15 (1972) 438 and 675;
G. Altarelli and G. Parisi, Nucl. Phys. 126 (1977) 297.

[3] E. A. Kuraev, L. N. Lipatov and V. S. Fadin, Sov. Phys. JETP 45 (1972) 199;
Y. Y. Balitsky and L. N. Lipatov, Sov. J. Nucl. Phys. 28 (1978) 822.

[4] A. H. Mueller, Nucl. Phys. B (Proc. Suppl.) 18 C (1991) 125.

[5] J. Kwieciński, A.D. Martin, P.J. Sutton, Phys. Rev. D46 (1992) 921.

[6] A.H. Mueller, Columbia preprint CU-TP-658 (1994).

[7] J. Bartels, H. Lotter, Phys. Lett. B309 (1993) 400.

[8] J. Bartels, A. De Roeck, M. Loewe, Z. Phys. C54 (1992) 635;
W.K. Tang, Phys. Lett. B278 (1992) 363.

[9] C.F. v. Weizsäcker, Z. Phys. 88, 612 (1934); E.J. Williams, Phys. Rev. 45 729.

[10] I.F. Ginzburg et al., Nucl. Inst. Meth. A205 (1983) 47, A219 (1984) 5;
V.I. Telnov, Nucl. Inst. Meth. A94 (1990) 72, Nucl. Phys. Proc. Suppl. 82 (2000) 359;
R. Brinkmann et al., Nucl. Instrum. Meth. A406 (1998) 13.

[11] V. Telnov, hep-ex/0101002 (2001).

[12] H1 Collab., C. Adolff et al. Nucl. Phys. B538 (1999) 3.

[13] ZEUS Collab., J. Breitweg et al., Eur. Phys. J. C6 (1999) 239.

[14] S. Catani and M. Seymour, Nucl. Phys. B485 (1997) 291.

[15] M. Seymour, Lund preprint LU-TP-94-12 (1994);
M. Seymour, Nucl. Phys. B436 (1995) 443

[16] G. Ingelman, Proc. of the HERA workshop, eds. W. Buchmüller and G. Ingelman, Hamburg (1991) vol. 3, p. 1366.

[17] J. G. Contreras, Phys. Lett. B 446 (1999) 158-162;
J.G. Contreras, R. Peschanski, C. Royon, Phys. Rev. D62 (2000)034006.

[18] J. Kwiecinski, A.D. Martin, J.J. Outhwaite Eur.Phys.J.C9:611-622,1999

[19] H. Jung, Nucl. Phys. Proc. Suppl. 79 (1999) 429.

[20] H. Jung, L. Jönsson, H. Küster, Eur. Phys. J. C9(1999) 383.

[21] H1 Collaboration, C. Adloff et al., Phys. Lett. B462 (1999) 440.

[22] J. Bartels, A. De Roeck and M. Loewe, Z. Phys. C 54 (1992) 635.

[23] W–K. Tang, Phys. Lett. B 278 (1992) 363.

[24] J. Kwiecinski, A. D. Martin and P. J. Sutton, Phys. Rev. D 46 (1992) 921.

[25] M. VGluck, E. Reya, and A. Vogt, Phys. Rev. D46 (1992) 1973.

[26] M. Boonekamp, A. De Roeck, C. Royon, S. Wallon, Nucl. Phys. B555 (1999) 540.